

<sup>11</sup>E. Wikborg and J. E. Inglesfield, *Solid State Commun.* **16**, 335 (1975).

<sup>12</sup>V. Sahni, J. B. Krieger, and J. Gruenebaum, *Phys. Rev. B* **15**, 1941 (1977).

<sup>13</sup>V. Sahni and J. Gruenebaum, *Solid State Commun.* **21**, 463 (1977).

<sup>14</sup>In Ref. 3  $B_{xc}$  is obtained from calculation of the energy in RPA; this is therefore the appropriate choice to compare with wave-vector analysis in RPA. In Ref.

5  $B_{xc}$  is obtained from expansion of the dielectric function  $\epsilon(Q)$ ;  $B_{xc}$  so obtained is *very* sensitive to choice of  $\epsilon(Q)$  [cf. D. J. W. Geldart, M. Rasolt, and R. Taylor, *Solid State Commun.* **10**, 279 (1972)], and does not correspond to any well-defined approximation such as RPA for the energy. In Ref. 5 a coefficient is also found for the *next*-order gradient correction from  $\epsilon(Q)$ , but this method neglects contributions in the same order  $\nabla^4$  of unknown size which arise in nonlinear response.

## Valence Band Structure of PbS from Angle-Resolved Photoemission

Thomas Grandke, Lothar Ley, and Manuel Cardona

*Max-Planck-Institut für Festkörperforschung, 7000 Stuttgart 80, Federal Republic of Germany*

(Received 25 January 1977)

The angular dependence of uv- (21.2-eV photon energy) induced photoemission from single-crystal PbS has been investigated. The dependence of the positions of observed peaks on  $k_{\parallel}$  is compared with the prediction of band-structure calculations. Nearly perfect agreement between theory and experiment is found by assuming that only peaks in the appropriate one-dimensional density of initial states calculated along lines of fixed  $k_{\parallel}$  contribute to the observed spectra.

The interpretation of angle-resolved photoelectron spectra (ARPES) in terms of electronic band structures suffers from the lack of information about the normal wave-vector component  $k_{\perp}$  of the photoexcited electron inside the crystal. Therefore, nearly all recent ARPES experiments<sup>1</sup> have been confined to layer compounds with  $k_{\perp}$  fixed in the direction normal to the layers; for such compounds, little or no energy dispersion is expected along  $k_{\perp}$ . Only a few exceptions<sup>2</sup> deal with "three-dimensional" crystals, and no straightforward and satisfying interpretation of the results has been given so far. In this Letter, we report the first ARPES measurements of PbS, which has the rock salt structure and a reasonably well-known band structure.<sup>3,4</sup> The positions of the peaks observed in the energy distribution spectra plotted versus the wave-vector component parallel to the crystal surface,  $k_{\parallel}$ , can be understood almost completely in terms of the one-dimensional density of states calculated along lines defined by  $\vec{k}_{\parallel} = \text{const}$  in reciprocal space.

The experiments were performed in a commercially available photoemission spectrometer described elsewhere.<sup>5</sup> The hemispherical electron analyzer was operated at a pass energy of 10 eV corresponding to a resolution of approximately 0.3 eV. The opening angle of the acceptance cone was 3°. A PbS single crystal was cleaved in vacuum along a (100) plane, the base pressure being

less than  $1 \times 10^{-10}$  Torr. Immediately after cleaving, the resulting surface was analyzed *in situ* by means of low-energy electron diffraction (LEED). Nearly the whole cleavage plane with an area of approximately 10 mm<sup>2</sup> exhibited the square LEED pattern of a perfect (100) surface of a face-centered cubic crystal. No evidence for surface disorder or surface reconstruction could be detected. The diffraction pattern preserved its sharpness for at least 48 h under ultrahigh-vacuum conditions. No changes were observed in the angle-resolved uv-induced photoemission spectra during this time either, confirming that the surface remained free of contaminants.

The orientation of the crystal was established inside the ultrahigh-vacuum chamber by means of its LEED pattern. The configuration used in the ARPES measurements described here was as follows: Designating the surface normal as the [100] direction, the electron acceptance cone was chosen to lie in the (010) plane. Consequently, the projection  $\vec{k}_{\parallel}$  of the electron momentum onto the surface was parallel to the [001] direction. All spectra were taken using the He I (21.2 eV) photons emitted by a differentially pumped resonance lamp. The incidence angle of the light,  $\theta_{\omega}$ , was kept constant at 45° whereas the electron acceptance direction varied from  $\theta = -28.5^{\circ}$  to  $\theta = +21.0^{\circ}$  in steps of mostly 1.5° (all angles refer to the surface normal).

In Fig. 1 we present some selected ARPES

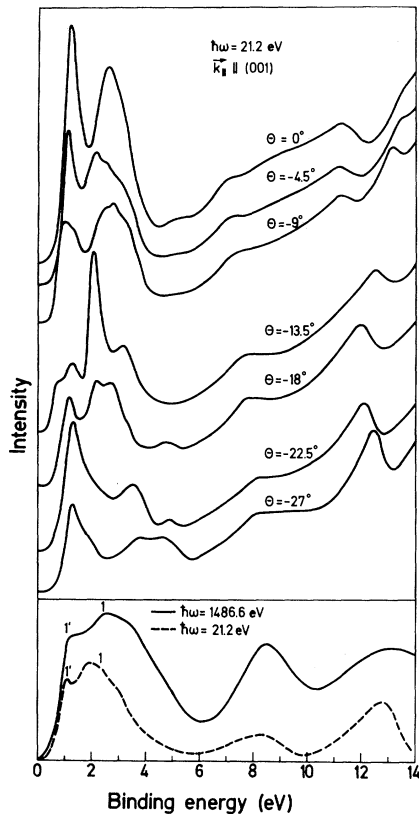


FIG. 1. Angle-resolved uv photoemission spectra, angle-integrated x-ray photoemission spectrum (Ref. 6), and uv photoemission spectrum (of polycrystalline PbS; Ref. 7). The zero of energies is taken at the position of the Fermi level.

spectra obtained at different angles  $\theta$ . For comparison, an angle-integrated x-ray photoemission (XPS) spectrum<sup>6</sup> and a rather similar uv photoemission (UPS) spectrum of polycrystalline PbS<sup>7</sup> are incorporated in the same figure. The most intense group of peaks in the ARPES spectra correspond to the peaks 1 and 1' in the XPS and UPS spectra. All other features in the ARPES spectra are much less prominent because of the low cross section of  $s$ -derived bands for uv photoexcitation. We therefore make no attempt to interpret them in terms of the band structure of PbS and focus on the  $p$ -derived valence bands within the first 5 eV binding energy.

Before comparing the ARPES spectra with the calculated band structure of PbS, we give a short outline of the theory of angle-resolved photoemission. The process of photoexcitation can be treated as the result of a transition between valence-band states and time-reversed (initial) states of the LEED problem.<sup>8</sup> Because of trans-

lational symmetry parallel to the surface, the LEED states are eigenstates of  $\vec{k}_{\parallel}$ , and this  $\vec{k}_{\parallel}$  must be conserved to a reciprocal-lattice vector (we assume, in agreement with the LEED pattern, no surface reconstruction). Because of the small penetration depth of these states into the solid, the final states are not eigenstates of  $k_{\perp}$  and conservation of this quantity plays no role in photoemission.<sup>8</sup>

We assume in the conventional manner that the transition-matrix elements are not strongly dependent on the energy of the initial state. This hypothesis is corroborated by the agreement between the angle-integrated XPS spectrum, the UPS spectrum of a polycrystalline sample, and the density of valence states of PbS.<sup>6,7</sup> We thus find for the angle-resolved photocurrent with electron energy  $E$  induced by photons of energy  $\omega$  (in atomic units) to be

$$I(E) \sim \iiint d^3k_v \delta(E_v + E - \omega) \delta(\vec{k}_{\parallel v} - \vec{k}_{\parallel}), \quad (1)$$

where  $\vec{k}_v$  is the crystal momentum of a valence-band state,  $\vec{k}_{\parallel v}$  the component of this momentum parallel to the surface,  $\vec{k}_{\parallel}$  the corresponding component of the photoelectron momentum, and  $E_v$  the energy (measured with respect to the vacuum level) of the valence-band state of momentum  $\vec{k}_v$ . The momentum  $\vec{k}_{\parallel}$  is related to  $E$  through

$$|\vec{k}_{\parallel}| = (2E)^{1/2} \sin \theta. \quad (2)$$

In Eq. (1) we avoid the use of reciprocal-lattice vectors of the two-dimensional translation lattice by working in the extended-zone scheme.

Two possible modes of measurement arise naturally. The easiest for the experiments, and the one used here, corresponds to keeping  $\theta$  constant. Theoretically, however, it is more convenient to treat the case in which  $\vec{k}_{\parallel}$  is kept constant: According to Eq. (2) this would correspond to varying  $\theta$  while the energy  $E$  is being swept. We treat this case first.

Since, for a given  $\theta$  and  $E$ ,  $\vec{k}_{\parallel}$  is fixed, only those valence electrons with  $\vec{k}_{\parallel v} = \vec{k}_{\parallel}$  contribute to the photocurrent. Thus, according to Eq. (1), the ARPES spectrum represents the density of states of the one-dimensional sections of the valence bands obtained by setting  $\vec{k}_{\parallel v} = \vec{k}_{\parallel}$ :

$$I(E, \vec{k}_{\parallel}) \sim [dE_v(\vec{k}_{\parallel v}, k_{\perp v})/dk_{\perp v}]_{E_v = \omega - E}^{-1}. \quad (3)$$

Equation (3) must be summed over all valence bands under consideration. In view of the sharp peaks associated with the singularities in the one-dimensional densities of states, we estimate that the condition  $\theta = \text{const}$ , used in our experiment,

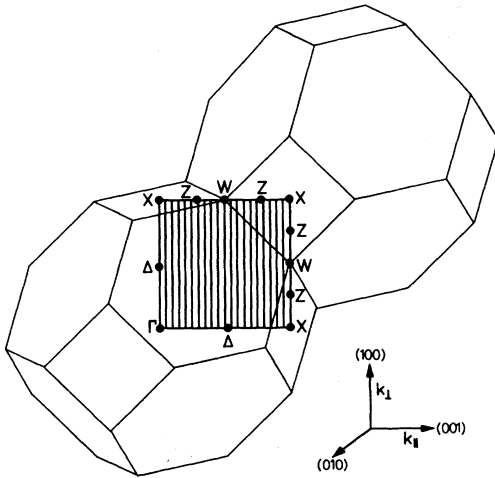


FIG. 2. Extended-zone scheme of the fcc structure. Our measurements were confined to irreducible wave vectors  $\vec{k}_v$  lying within the square  $X-X-X-\Gamma$ . One-dimensional densities of states were calculated along  $\vec{k}_{\parallel v} = \text{const}$ , as indicated by the vertical lines.

does not significantly shift the peaks in an ARPES spectrum.

We point out that the results of Eq. (3) will be modulated by a transition probability which is assumed to be weakly dependent on energy. The correctness of this assumption is justified because in our experiments we only see peaks related to singularities in the one-dimensional density of states of Eq. (3). The small width of only  $\sim 0.1$  eV of these singularities ensures negligible shifts of these structures due to a slowly varying transition probability. It can happen, however, that this transition probability is zero (no final states available for the transitions); in this case, the corresponding structure in the ARPES spectrum disappears.

The positions of lines in reciprocal space defined by  $\vec{k}_{\parallel v} = \vec{k}_{\parallel} = \text{const}$  depend on the specific orientation of the investigated crystal relative to the electron analyzer. In Fig. 2 we have sketched the irreducible parts of these lines, within the extended-zone scheme of an fcc crystal, which corresponds to our experimental situation. The one-dimensional density of states along these lines was calculated according to Eq. (3). For the computation of the energy bands  $E(\vec{k}_v)$ , we have utilized the empirical pseudopotential method and the pseudopotential coefficients given by Kohn *et al.*<sup>3</sup> For simplicity we have neglected the spin-orbit interaction which causes splittings of about 0.25 eV in the valence bands of PbS.<sup>3,9</sup>

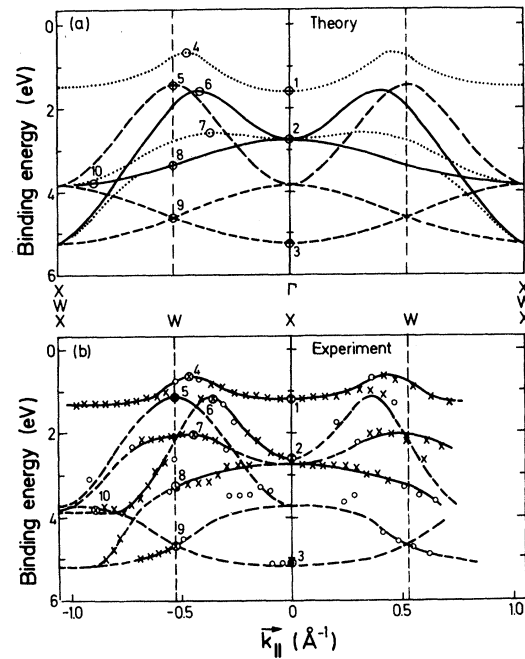


FIG. 3. (a) Dependence of the energies of critical points in the one-dimensional density of states on  $\vec{k}_{\parallel v}$ . The solid lines refer to critical points at  $k_{\perp v} = 0$ , the dashed lines to critical points at  $k_{\perp v} = 2\pi/a$ , and the dotted lines to critical points at an intermediate value of  $k_{\perp v}$ . (b) Peak positions vs electron momentum component  $\vec{k}_{\parallel}$ . The experimental points are connected by lines to give energy-vs-momentum curves similar in shape to those of (a). The experimental and calculated energies of ten selected points (marked 1 to 10) are compared in Table I.

The energy dependence of the maxima in  $I(E)$  as given by Eq. (3) as a function of  $\vec{k}_{\parallel v}$  is plotted in Fig. 3(a) for the upper valence bands, mainly derived from the  $3p$  levels of sulfur. We note that full lines correspond to critical points located at  $k_{\perp v} = 0$  (i.e., along the line  $\Gamma-\Delta-X$ ), dashed lines to critical points at  $k_{\perp v} = 2\pi/a$  (i.e., along the lines  $X-Z-W-Z-X$ ), and dotted lines to critical points at some intermediate value of  $k_{\perp v}$ .

In Fig. 3(b) we have plotted the peak positions  $E$  versus the corresponding electron momentum component  $\vec{k}_{\parallel}$ . The crosses stand for intense peaks in the ARPES spectra, while the open circles refer to weak peaks or shoulders. First, we emphasize that it is possible to connect these discrete points by continuous lines very similar in shape to those of Fig. 3(a). Thereby we are able to assign every observed peak to a critical point in the one-dimensional density of initial states.

In Table I we compare the experimental and

TABLE I. Comparison of the energies of selected features in the experimental and calculated  $E$ -vs- $\vec{k}_{\parallel}$  curves. The numbers 1 to 10 refer to Fig. 3. Energies are given relative to the top of the valence bands.

No.	Symmetry designation	$E$ (eV)	
		Experimental	Calculated
1	$\Delta_7$	1.20	1.60
2	$\Gamma_6^-, \Gamma_8^-$	2.70	2.80
3	$\Gamma_6^-$	5.20	5.25
4	...	0.65	0.70
5	$W_6$	1.10	1.45
6	$\Delta_7$	1.20	1.60
7	...	2.05	2.60
8	$\Delta_6$	3.40	3.40
9	$W_6, W_7$	4.70	4.65
10	...	3.80	3.80

calculated energies of some representative features of the  $E$ -vs- $\vec{k}_{\parallel}$  curves marked 1 to 10 in Fig. 3. The splittings of 0.2 eV at point  $\Gamma$  around 2.7 eV and at  $|\vec{k}_{\parallel}| = 0.75 \text{ \AA}^{-1}$  around 3.7 eV binding energy are attributed to the spin-orbit interaction neglected in our calculation. We believe that the agreement between theory and experiment shown in Table I is within what can be expected for the accuracy of any band-structure calculation. Some minor disagreements occur around  $|\vec{k}_{\parallel}| = \pm 0.25 \text{ \AA}^{-1}$ , where weak shoulders that appear apparently do not correspond to any calculated critical point. The absence of about 30% of the predicted peaks is attributed to the absence of appropriate final states. This problem

could be circumvented by using several different photon energies (e.g., with synchrotron radiation).

Finally, we stress the importance of using the one-dimensional density of states instead of single symmetry lines coinciding with the direction of the experimental  $\vec{k}_{\parallel}$  for interpreting the ARPES spectra. This is especially true for the highest observed peak that cannot be explained by only using the band structure along the lines  $\Gamma-\Delta-X$  and  $X-Z-W-Z-X$ .

We thank M. L. Cohen for supplying us with the form factors needed for the band-structure calculation and G. Krutina and W. Neu for their technical assistance.

<sup>1</sup>See, e.g., N. V. Smith, M. M. Traum, and F. J. Di Salvo, *Solid State Commun.* **15**, 211 (1974); P. K. Larsen, G. Margaritondo, J. E. Rowe, M. Schlüter, and N. V. Smith, *Phys. Lett.* **58A**, 423 (1976).

<sup>2</sup>See, e.g., N. V. Smith and M. M. Traum, *Phys. Rev. Lett.* **31**, 1247 (1973); P. M. Williams, P. Butcher, J. Wood, and K. Jacobi, *Phys. Rev. B* **14**, 3215 (1976).

<sup>3</sup>S. E. Kohn, P. Y. Yu, Y. Petroff, Y. R. Shen, Y. Tsang, and M. L. Cohen, *Phys. Rev. B* **8**, 1477 (1973).

<sup>4</sup>P. J. Lin and L. Kleinman, *Phys. Rev.* **142**, 478 (1966).

<sup>5</sup>T. Grandke and L. Ley, to be published.

<sup>6</sup>F. R. McFeely, S. Kowalczyk, L. Ley, R. A. Pollak, and D. A. Shirley, *Phys. Rev. B* **7**, 5228 (1973).

<sup>7</sup>M. Cardona, D. W. Langer, N. J. Shevchik, and J. Tejada, *Phys. Status Solidi (b)* **58**, 127 (1973).

<sup>8</sup>P. J. Feibelman and D. E. Eastman, *Phys. Rev. B* **10**, 4932 (1974).

<sup>9</sup>F. Herman, R. L. Kortum, I. B. Ortenburger, and J. D. van Dyke, *J. Phys. (Paris)*, *Colloq.* **29**, C4-62 (1968).